HHS Public Access

Author manuscript

*Med Mycol*. Author manuscript; available in PMC 2016 June 01.

Published in final edited form as:

*Med Mycol*. 2015 June ; 53(5): 493–504. doi:10.1093/mmy/myv012.

# Morphology and its underlying genetic regulation impact the interaction between *Cryptococcus neoformans* and its hosts

**Jianfeng Lin**[1,2], **Alexander Idnurm**[2,3,*], and **Xiaorong Lin**[1,*]

[1]Department of Biology, Texas A&M University, College Station, Texas, USA

[2]School of Biological Sciences, University of Missouri-Kansas City, Missouri, USA

[3]School of BioSciences, University of Melbourne, Melbourne, Victoria, Australia

## Abstract

*Cryptococcus neoformans* is a fungus that causes the majority of fatal cryptococcal meningitis cases worldwide. This pathogen is capable of assuming different morphotypes: yeast, pseudohypha, and hypha. The yeast form is the most common cell type observed clinically. The hyphal and pseudohyphal forms are rarely observed in the clinical setting and are considered attenuated in virulence. However, as a ubiquitous environmental pathogen, *Cryptococcus* interacts with various organisms, and it is known to be parasitic to different hosts. Capitalizing on recent discoveries, morphogenesis regulators were manipulated to examine the impact of cell shape on the cryptococcal interaction with three different host systems: the soil amoeba *Acanthamoeba castellanii* (a protist), the greater wax moth *Galleria mellonella* (an insect), and the murine macrophage cell line J774A.1 (mammalian cells). The regulation of Ace2 and morphogenesis (RAM) pathway is a highly conserved pathway among eukaryotes that regulates cytokinesis. Disruption of any of five RAM components in *Cryptococcus* renders cells constitutively in the pseudohyphal form. The transcription factor Znf2 is the master activator of the yeast to hyphal transition. Deletion of *ZNF2* locks cells in the yeast form, while overexpression of this regulator drives hyphal growth. Genetic epistasis analyses indicate that the RAM and the Znf2 pathways regulate distinct aspects of cryptococcal morphogenesis and independently of each other. These investigations using the *Cryptococcus* RAM and *ZNF2* mutants indicate that cell shape, cell size, and likely cell surface properties weigh differently on the outcome of cryptococcal interactions with different hosts. Thus, certain traits evolved in *Cryptococcus* that are beneficial within one host might be detrimental when a different host is encountered.



*To whom correspondence should be addressed. Xiaorong Lin. Department of Biology, Texas A&M University, College Station, TX 77843-3258. Tel: +979-845-7274; Fax: +979-845-289; xlin@bio.tamu.edu, Alexander Idnurm. School of BioSciences, University of Melbourne, Victoria, VIC 3010, Australia. Tel: +61 (03) 8344 2221; Fax: +61 (03) 9347 5460; alexander.idnurm@unimelb.edu.au.

**Supplementary material**

Supplementary material is available at *Medical Mycology* online (http://www.mmy.oxfordjournals.org/).

**Declaration of interest**

The authors report no conflicts of interest. The authors alone are responsible for the content and the writing of the paper.

**Keywords**

morphogenesis; amoeba; macrophage; greater wax moth; phagocytosis; hyphae; pseudohyphae; mating

## Introduction

Morphological changes are fundamental to the ability of fungi to cause disease in plants and animals. For medically relevant species, it is evident that disrupting the ability to change cell shape results in loss of pathogenicity, illustrated by work in dimorphic species in which strains locked into one cell form have impaired ability to cause disease [1,2]. However, in many fungi it is still not clear what advantages some alternative cell morphologies provide or if they come at a fitness cost to the organism.

*Cryptococcus neoformans* is the major etiological agent of cryptococcal meningitis, a fatal disease that has been estimated to kill more than 600,000 people worldwide each year [3]. However, as a ubiquitous environmental pathogen, the encounter of this fungus with a susceptible mammalian host is accidental. Therefore, many virulence traits in this pathogen are postulated to be selected through its interaction with the environment or its natural predators. These virulence traits include encapsulation, melanization, and thermotolerance [4]. These traits are beneficial to this pathogen under natural conditions and also during infection in a mammalian host and are thus considered “dual use” factors [5]. Besides the aforementioned traits, cell morphotype also plays an important role in cryptococcal virulence (see reviews [6,7] and references therein), similar to what has been demonstrated in many other environmental fungal pathogens [8]. However, most of the information on the impact of cryptococcal morphotype on its interaction with different hosts was obtained with natural isolates [9]. The difference in the genotype of isolates used as well as the underlying mechanisms responsible for the morphological changes complicates the interpretation of these studies. Critical genetic components controlling cryptococcal morphotypes have been identified in the past few years (as detailed below), making it now possible to conduct comparative analyses using cryptococcal strains in the same genetic background, carrying different mutations, and with different morphological forms.

Three morphotypes can occur in *C. neoformans*: yeast, pseudohypha, or hypha. Enlarged yeast cells have also been characterized [10-12]. The fungus typically grows as a haploid yeast. The morphological transition from the yeast form to the hyphal form takes place during both bisexual mating (**a**-α mating) and unisexual mating (mostly $\alpha$-α mating) [13-19]. Non-mating stimuli can also trigger hyphal growth [20-22]. Regardless of the upstream stimuli, the zinc-finger transcription factor Znf2 is a key regulator for hyphal growth (Fig. 1A). Deletion of the *ZNF2* gene restricts *Cryptococcus* in the yeast form [20,23,24], whereas elevated expression of *ZNF2* drives hyphal growth irrespective of environment stimuli or mating type [20,24,25]. Consistent with earlier observations of a reversed relationship between filamentation and virulence (see review [6] and references therein), the *znf2*Δ mutant in H99 background that is locked in the yeast form is more

virulent than the wild-type, while the strain with overexpression of the *ZNF2* gene is incapable of causing fatal infection in mice [23,26].

*Cryptococcus* can assume the pseudohyphal growth form in response to nutrient limitation [6,27]. Disruption of the RAM pathway, however, renders this fungus in the pseudohyphal form constitutively [28]. The RAM pathway is a conserved signal transduction network among eukaryotes [29], and it has been shown to impact numerous cellular processes, such as in the best-studied species *Saccharomyces cerevisiae* to include cell cycle regulation [30,31], cell separation [32-35], mating [32,34], and cell polarization [33,35]. Similar to the RAM pathway in *S. cerevisiae*, the RAM pathway in *C. neoformans* is composed of two serine/threonine protein kinases, Cbk1 and Kic1, and three associated proteins, Mob2, Tao3, and Sog2 (Fig. 1A) [28,36]. Tao3 is likely the scaffold protein in the RAM pathway [28,32,33,36], and Mob2 functions as a Cbk1- regulatory subunit [37]. Hym1, a RAM pathway component that physically associates with Kic1 in *S. cerevisiae*, has not been identified as a RAM component in *C. neoformans* [28]. The downstream targets of the RAM pathway (i.e., of the Cbk1 kinase) in *Cryptococcus* remain elusive. There is no cryptococcal homolog of Ace2, one downstream target of the RAM pathway found in *S. cerevisiae* and *S. pombe* [28]. Cryptococcal mutants in the RAM pathway (*tao3*, *mob2*, *kic1*, *cbk1*, and *sog2*) all have the same pseudohyphal phenotype [28]. In some strain backgrounds they are temperature-sensitive [28,36]. When both mating partners harbor the same mutation, they failed to produce mating filaments or meiotic basidiospores. Mutations in the RAM pathway also drastically attenuate cryptococcal virulence [36].

Thus, both hyphae and pseudohyphae are morphological forms that are attenuated for virulence during *Cryptococcus* infection in a mammalian host (mouse). This reduction in virulence could be due to the inherent property of these morphological forms where the physical interconnections between cells prevent the fungus from extrapulmonary dissemination and consequently from causing fatal brain infections. Indeed, neither the $ZNF2^{oe}$ strain nor a RAM mutant in the H99 background could be detected in the brain tissue, although both were present in the lungs during infection [36,38]. Given that *Cryptococcus* likely disseminates to the brain at least in part through a Trojan horse mechanism after being phagocytosed by host cells [39-41], it would be interesting to test if morphotype affects phagocytosis of cryptococcal cells. The pseudohyphal form was isolated as being resistant to phagocytosis by soil amoebae in the 1970s [9]. These natural pseudohyphal isolates were later found to habor mutations in the RAM pathway [28]. It is not known if the hyphal form of *Cryptococcus* is also resistant to the phagocytosis by soil amoebae and if common factors affect phagocytosis of the two filamentous forms of *Cryptococcus* by amoebae, wax moth, and mammalian phagocytes.

In this study, we tested if the RAM pathway and the Znf2 pathway regulate independent or common aspects of cryptococcal morphogenesis based on genetic epistasis analyses. To investigate the impact of morphotype on cryptococcal interaction with different hosts, we used the RAM and *ZNF2* mutants (single and double mutants) that grow in different morphological forms and tested three different host systems: the soil amoeba *Acanthamoeba castellanii* (a protist), the wax moth *Galleria mellonella* (an insect), and the murine macrophage cell line J774A.1 (mammalian cells). Our results indicate that cell shape

(polarized form vs yeast form) weigh differently on the outcome of the interaction between *Cryptococcus* and different hosts. Thus, certain traits evolved in *Cryptococcus* that are beneficial against one predator might be detrimental when a different host is encountered, and the effect of morphotype is host- and condition-specific.

## Methods and materials

### Strains, growth conditions, and morphological examination

Strains used in this study are listed in Table S1. The recombinant progeny between RAM pathway gene mutations and *ZNF2* alleles were isolated from crosses, and their mating types and genotypes were confirmed by phenotypic assays and polymerase chain reaction (PCR). All *C. neoformans* cells were maintained on yeast peptone dextrose (YPD) medium or YPD + $Cu^{2+}$ (20 μM) for the $P_{CTR4–2}$-*ZNF2* strain at 30°C, unless stated otherwise. For crosses to test for amoebic predation, **a** and $\alpha$ mating pairs with equal number of cells (five microliters each at the cell concentration of $1.5 \times 10^7$ cells/ml) were cultured together on V8 agar medium in the dark at 22°C. Hallmarks of successful mating, including the formation of mating hyphae and spores, were examined using an Olympus SZX 16 stereoscope.

For morphological examination, the wild-type and the mutant strains were inoculated into liquid media of YPD, YPD+copper (20 μM), or YPD+ bathocuproinedisulfonic acid (BCS; 200 μM) with the initial $OD_{600}$ being 0.1. After 60 hours of standing incubation, cellular morphology of these strains was examined under an Olympus CX41 light microscope. Images of these cells were captured using the QCapture software.

### Murine macrophage phagocytosis assay

Mouse macrophage cell line J774A.1 (ATCC® TIB-67™) was acquired from the American Type Culture Collection, along with the ATCC-formulated Dulbecco's Modified Eagle's Medium (DMEM, catalog no. 30-2002). Fetal bovine serum (FBS) was added into DMEM to a final concentration of 10% immediately prior to the incubation. Three hundred microliters of freshly grown J774A.1 cells were seeded into 24 well microtiter plates, with $2.5 \times 10^5$ cells per well. The macrophage cells were cultured at 37°C with 5% $CO_2$ overnight. Old culture media were then replaced by refresh DMEM with 10% FBS. *Cryptococcus* cells of $2.5 \times 10^6$ or more were introduced to each well for the phagocytosis assay. After 30 s of rock mixing, the co-cultures were incubated at 37°C with 5% $CO_2$ for an additional 2 hours. The co-cultures were then washed three times with warm phosphate buffered saline (PBS; 500 μl/well/time) to remove medium and non-adherent cells before fixed with 300 μl 10% formaldehyde made in PBS.

For the prestaining approach, *Cryptococcus* cells were stained with calcofluor white (20 μg/mL) for 5 minutes before the infection. For the post-stain approach, calcofluor white was used to stain the cells after phagocytosis, and then cells were fixed. The rest of the experiments were performed the same way as described in the previous paragraph. The cells were examined under an inverted microscope (Eclipse Ti, Nikon), and the images were captured using the NIS elements AR 3.0 software.

### Amoebic predation assays

*Acanthamoeba castellanii* (ATCC® 30234™) purchased from ATCC was stored and grown in the PYG medium (ATCC® media 712) as described on the product sheet supplied by ATCC. In brief, 0.25 ml peak density (about 2 weeks growth) culture was transferred into 5 ml fresh PYG liquid media and incubated at 22°C with a 15° horizontal slant.

For the predation assay, the agar plates were cultured for 60 hours with a lawn of cryptococcal cells (original inoculum per plate: 250 μl of a culture with $OD_{600}$ = 0.5). A 5–10 μl aliquot of a week old amoebic culture ($OD_{600} \approx 0.8$) was dropped onto the center of the cryptococcal lawn. The diameter of the predation halo on each plate was recorded daily. Each strain had three replicates. The amoebic predation zone was defined as Dt–D0 (the diameter on the day of recording subtract the initial diameter). Because the predation zone was not in a perfectly round shape, the diameter of the predation zone was defined as the average of diameters measured with 8 different directions (see Supplemental Fig. 1 for the diagram). The amoebic predation zone was then plotted against the time using the program OriginPro 8.6.

For the amoebic predation assay on mating colonies, the mating pair was first cultured together for a week to allow the mating hyphae to be generated before dropping an aliquot of the amoeba culture on top of the mating colony. Instead of measuring the predation diameter, the amoebic cell number recovered from each cryptococcal mating colony after 2–3 weeks of co-incubation was counted using a hemocytometer.

### *Galleria mellonella* infection

*Galleria mellonella* at the final instar larval stage were purchased from Vanderhorst Wholesale Inc. The greater wax moth infection experiments were performed as described previously [42]. *C. neoformans* strains were grown overnight in YPD+BCS (200 μM) liquid medium. Cells were washed three times with PBS and then resuspended in PBS buffer to the final concentration of $OD_{600}$ = 1. Using a 10μl Hamilton syringe, 5 microliters of *Cryptococcus* cells (~$5 \times 10^4$ yeast cells) were injected into *G. mellonella* hemocoel through the last left proleg, and the control group was injected with 5 microliters of sterile PBS. Before injection, the area was cleaned using an alcohol swab. After 4 hours of incubation at 30°C, the haemolymph of infected larvae (~5 μl) was collected into 45 μl anti-agglutination buffer *via* gentle squeezing of a cut at the proleg as described previously [43]. The haemolymph material containing haemocytes and fungal cells were then examined microscopically.

## Results

### The RAM pathway and the Znf2 pathway control distinct aspects of morphogenesis

To investigate the relationship between the RAM pathway and the Znf2 pathway, we crossed the *znf2*Δ mutant or the conditional *ZNF2* overexpression strain ($P_{CTR4\text{-}2}$-*ZNF2*) with the RAM mutants (*tao3*Δ, *mob2*Δ, *kic1*Δ, *cbk1*Δ, and *sog2*Δ). In the $P_{CTR4\text{-}2}$-*ZNF2* strain, the expression of *ZNF2* is driven by the promoter of the *CTR4* gene that encodes a copper transporter [44]. The expression of *ZNF2* is thus suppressed by copper and induced

by copper starvation in the presence of copper chelator bathocuproinedisulfonic acid (BCS) [20,25]. The isolated double mutants were examined for their morphology and other phenotypes. We found that mutations in the different RAM components in these double mutants conferred the same phenotypes (data not shown), consistent with their established role in one complex [28,36]. Thus, for the following experiments, we chose to use strains with the deletion in the gene encoding the kinase Cbk1 to represent the RAM complex (Fig. 1A).

To compare the morphology of the single and double mutants, we cultured the strains in YPD liquid medium with or without supplementation of copper or BCS. As expected, the wild-type H99 strain and the *znf2*Δ mutant showed the yeast morphotype under these conditions (Fig. 1B). The *cbk1*Δ mutant grew in the pseudohyphal form (Fig. 1B). The $P_{CTR4\text{-}2}$-*ZNF2* strain grew strictly in the yeast form in the YPD+copper medium, but it became filamentous in the YPD+BCS medium when the expression of *ZNF2* was induced (Fig. 1B). Although the majority of the $P_{CTR4\text{-}2}$-*ZNF2* cells were in the yeast form in the YPD medium, a few cells became filamentous during prolonged incubation, likely due to the increasingly limited copper level in the medium. It is known that the YPD medium is copper-limiting; for example, growth of the cryptococcal strain defective in the copper regulator Mac1/Cuf1 is poor in this medium [19]. The double mutant *cbk1*Δ *znf2*Δ had the same pseudohyphal morphotype as the single *cbk1*Δ mutant. Interestingly, the *cbk1*Δ $P_{CTR4\text{-}2}$-*ZNF2* strain grew in the hyphal form when the expression of *ZNF2* was induced (YPD+BCS). The hyphal production caused by the induction of *ZNF2* in the *cbk1*Δ mutant background was more robust than the expression of *ZNF2* alone in the wild-type background (Fig. 1B). We speculate that driving hyphal growth from pseudohyphae might be a more efficient process than switching to hyphal growth from yeast growth. The length of the hyphae increased over time in this *cbk1*Δ $P_{CTR4\text{-}2}$-*ZNF2* strain under the inducing condition (Fig. 1C). In addition, these results show that the mating defect of the RAM mutants is not due to an impediment in their capabilities for filamentous development. These observations also indicate that the mutations in *znf2* and *cbk1* have somewhat complicated genetic interactions: $ZNF2^{oe}$ is epistatic over *cbk1*Δ in hyphal formation, while *cbk1*Δ is epistatic over *znf2*Δ for pseudohyphal formation. However, they show that the two pathways control distinct morphotype generation and that they act independently based on the phenotypes of the double mutants.

## Murine macrophage cells can phagocytose yeasts and hyphae but not pseudohyphae

Although the $ZNF2^{oe}$ strain with constitutive activation of *ZNF2* is avirulent in the murine model of cryptococcosis, that strain could persist and amplify in the animal lungs during the first two weeks of infection [23]. A RAM mutant is also significantly attenuated in mouse model, but it can persist in the lungs even after 70 days post infection [36]. This is somewhat surprising given that the RAM mutants used in that experiment grow less well at 37°C *in vitro* [28,36]. Interestingly, neither the $ZNF2^{oe}$ strain nor the RAM mutant causes infections in the brain, despite their presence in the lungs [23,36]. As a Trojan horse mechanism is important for this facultative intracellular pathogen to spread systemically and to invade the brain [39-41], we hypothesized that the filamentous morphotype (pseudohyphae or hyphae) might be blocked in dissemination from the lungs due to lack of phagocytosis.

To examine the impact of morphotype on the phagocytosis of *Cryptococcus* by murine macrophages, we infected the J774A.1 cell line with *Cryptococcus* cells including the wild-type H99 (yeast), the *cbk1*Δ mutant (pseudohyphae), and the $P_{CTR4\text{-}2}$-*ZNF2* strain precultured under the inducing condition (hyphae). After 2 hours of co-incubation, cells were washed with PBS and fixed with formaldehyde. To distinguish extracellular from intracellular cryptococcal cells, we stained the cells with calcofluor white after phagocytosis (post-stain). Calcofluor white is a fluorochrome that binds chitin in the fungal cell wall [45] and it stains extracellular cryptococcal cells. As expected, we found both intracellular yeast cells and adherent extracellular yeast cells of the wild type (Fig. 2B), consistent with *Cryptococcus* being a facultative intracellular pathogen [46]. To our surprise, some hyphae produced by the $P_{CTR4\text{-}2}$-*ZNF2* strain were also phagocytosed (Fig. 2D), although the efficiency of hyphal phagocytosis was only half of that for yeasts (Fig. 2G). By contrast, no pseudohyphae of the *cbk1*Δ mutant were found either intracellularly or extracellularly (Fig. 2F). To confirm that we did not miss any hidden cryptococcal cells, we cultured *Cryptococcus* with calcofluor white prior to the co-culture with J774A.1 cells (pre-stain). After 2 hours of co-culturing, cells were again washed with PBS and fixed with formaldehyde. This approach allows the clear visualization of cryptococcal cells, either intracellular or extracellular. Again, both intracellular and adherent extracellular yeast cells (H99) and hyphae ($P_{CTR4\text{-}2}$-*ZNF2*) were observed (Fig. 2A, C). Consistent with our post-stain approach, we did not find any *cbk1*Δ mutant pseudohyphae cells (Fig. 2E, 2F). Taken together, the results indicate that the murine macrophage can engulf yeast and hyphae, but not pseudohyphae.

## The hyphal and pseudohyphal, but not the yeast, forms of *Cryptococcus* are resistant to predation by amoebae

The soil amoeba is proposed to act as one of the selective pressures for the evolution of virulence traits in *C. neoformans* [36,47-49]. Prior observations indicate that the pseudohyphal RAM mutants are resistant to amoebic predation [9,28]. Given the differences that we observed for the hyphae and pseudohyphae in the murine macrophage assays, we decided to examine the impact of morphotype as controlled by Znf2 expression on cryptococcal resistance to amoebic predation.

We designed the following approach to assay amoebic predation. We first cultured a lawn of cryptococcal cells on an agar plate and then dropped the amoebic culture onto the center of the plate. The impact of the predation by amoebae is reflected by the clear zone expanded from the center (Supplemental Fig. 1A). Conditions that favored rapid amplification of *Cryptococcus* (YPD and PYG media) were not suitable for the detection of amoebic predation (Supplemental Fig. 1B). In comparison, amoebic predation of *Cryptococcus* on nutrient-limiting V8 juice agar was easily detectable (Supplemental Fig. 1B).

We performed the amoebic predation assay with the wild-type H99 strain, the *cbk1*Δ mutant, the *znf2*Δ mutant, and the $P_{CTR4\text{-}2}$-*ZNF2* strain on V8 medium with or without the addition of copper or BCS. Consistent with previous results [9,36], the *cbk1*Δ RAM mutant was highly resistant to the predation by amoebae, and no expansion of the predation zone was detected even after 3 weeks of incubation (data not shown). We found cryptococcal

pseudohyphal cells and amoebic cysts at the original inoculation sites, indicating that the pseudohyphal cells can indeed survive the amoebic predation under the tested conditions (data not shown). Amoebae predated the wild-type H99 strain and the *znf2*Δ mutant similarly well on these media (Fig. 3A), both strains were in the yeast form under these tested conditions. Likewise, amoebae predated the $P_{CTR4\text{-}2}$-*ZNF2* strain as well as the wild-type H99 on V8 medium or V8+copper medium (Fig. 3A and Supplemental Fig. 1C). By contrast, the expansion of the amoebic predation zone on this $P_{CTR4\text{-}2}$-*ZNF2* strain on the V8+BCS medium (with *ZNF2* induction) was drastically slower (Fig. 3A and Supplemental Fig. 1C). We then used microscopy to examine closely three areas on this plate: the area outside of the predation zone, the border of the predation zone, and the area inside the predation zone. The $P_{CTR4\text{-}2}$-*ZNF2* strain formed yeast colonies mixed with hyphae extending in all directions on V8+BCS medium (Fig. 3B). At the border and inside the predation zone, yeast cells were being dismantled by amoebae, with hyphae being the "leftovers" (Fig. 3B). Further examination of the $P_{CTR4\text{-}2}$-*ZNF2* strain under a compound microscope revealed that amoebae engulfed and digested the yeast cells (Fig. 3C). By contract, amoebae only wrapped around hyphae and the hyphae being attacked were still viable (Fig. 3C). Thus, the cells of the same genetic makeup displayed difference in their resistance to amoebic predation due to their morphological difference.

The aforementioned results suggest that amoebae preferentially engulf yeast cells and leave behind hyphae or pseudohyphae. It is known that spontaneous mutations in the RAM pathway genes can occur relatively frequently under natural conditions and the reversion of these mutations also occur under conditions that select against the pseudohyphal form [36,38]. Thus resorting to loss of RAM pathway signaling is a reasonable approach for *Cryptococcus* to resist the predation by amoebae. *Cryptococcus* is also known to naturally upregulate *ZNF2* and undergoes morphological transition from the yeast growth to hyphal growth during mating [14,15].

The experiments described thus far used transgenic *Cryptococcus* strains to investigate the role of morphologywith different host organisms. Naturally formed mating hyphae of wild-type cells were then tested in amoebic predation assays. Mating colonies were formed by two pairs of wild-type strains: the serotype A (var. *grubii*) wild-type congenic pairs H99α and KN99**a** [50] and the serotype D (var. *neoformans*) congenic pairs XL280α and XL280**a** [24]. We included their corresponding *znf2*Δ **a** and $\alpha$ strains as a control. It is known that *znf2*Δ mutants are capable of mating but they are specifically blocked in the hyphal morphogenesis [32]. As shown in Figure 4, the serotype D XL280α-XL280**a** pair mated robustly and produced abundant hyphae that gave the white fluffy appearance to the mating colony. The serotype A H99α-KN99**a** pair also mated and produced spotty hyphae at the periphery of the colony. As expected, the *znf2*Δ mutant mating colonies remained in the yeast form (Fig. 4A). After the addition of amoebae, the yeast cells in the center of the H99α-KN99**a** mating colony were cleared by amoebae. The corresponding non-filamenting mating colony of the H99 *znf2*Δ mutants was completely destroyed. Accordingly, more amoebic cells were recovered from the *znf2*Δ mutant mating colony than those from the wild-type mating colony (Fig. 4B), most likely due to access to more digestible food source (yeast cells). Very minimal impact was observed on the XL280α-XL280**a** mating colony,

where filamentation was much more robust compared to the serotype A (Fig. 4A). Again, increased predation on the XL280 *znf2*Δ mutant mating colony was observed compared to the wild-type control (Fig. 4A, B). Interestingly, amoebae made a much more modest impact on the XL280 background compared to the H99 background, even for the *znf2*Δ mutant (Fig. 4B). This suggests that other genetic factors, in addition to morphotype, also influence the efficiency of amoebic predation.

Collectively, the findings presented here indicate that hyphae and pseudohyphae are resistant to the amoeba *A. castellanii* while yeast cells, even genetically identical to the filamentous cells, are susceptible to this soil microbial hunter.

## Hyphae and pseudohyphae elicit haemocyte nodulation during *Galleria mellonella* infection

*Galleria mellonella* (the greater wax moth) has been used as an alternative host system to assess *C. neoformans* virulence traits. For example, the classic factors important for cryptococcal virulence in mammalian models, like melanin and capsule synthesis, were shown to be important also in the *G. mellonella* model [42]. Although insects do not have adaptive immune systems as mammals do, they do have sophisticated innate immune responses, including for pathogen recognition, production of antimicrobial peptides, and the formation of a multicellular complex to encapsulate invading pathogens [51-53]. Haemocytes are the major cellular defense mediator in the *G. mellonella* haemolymph and they are functionally equivalent to macrophages and neutrophils in mammals [52]. Haemocyte aggregation (haemocyte nodulation) is one of the most important defense systems in insects to contain foreign invaders [54,55]. Previous studies demonstrate that the pseudohyphal RAM mutants are attenuated in virulence in the *G. mellonella* model [36]. Here, we decided to analyze the impact of morphotype on the cellular responses of *G. mellonella* against *Cryptococcus*.

We infected *G. mellonella* with the wild-typeH99 strain, the $P_{CTR4\text{-}2}$-*ZNF2* strain, the *cbk1*Δ mutant, the *cbk1*Δ $P_{CTR4\text{-}2}$-*ZNF2* strain, or the PBS control. All cryptococcal strains were precultured overnight in YPD+BCS medium to induce hypha production in strains that contain the $P_{CTR4\text{-}2}$-*ZNF2* construct (Fig. 1C). Haemolymph samples were collected from infected larvae four hours after the injection, and they were immediately examined microscopically for haemocyte nodulation [43,47,56]. All strains elicited *Galleria* cellular immune responses, as haemocyte nodulation was detected for all of them (Fig. 5). However, pseudohyphae and hyphae induced much stronger responses than yeast cells (Fig. 5). At higher magnification, we found that yeast cells (H99) were phagocytosed by haemocytes, and there was a minute level of clustering of haemocytes compared to the PBS control. By contrast, hyphae and pseudohyphae caused large clustering of haemocytes, with many layers of haemocytes wrapped around the filamentous cryptococcal cells (Fig. 5). This effective containment of hyphae and pseudohyphae by haemocyte nodulation likely contribute to this insect's resistance to the nonyeast forms.

## Discussion

The results presented in this study demonstrate the importance of morphotype in shaping the interaction between *Cryptococcus* and various hosts. Both hyphae and pseudohyphae confer resistance to the predation by soil amoebae (Table 1). Thus, being in a filamentous form is beneficial to *Cryptococcus* in defending itself against this single-celled protist. Similarly, both hyphae and pseudohyphae are resistant to phagocytosis by haemocytes during infection in the greater wax moth. In the wax moth, however, haemocyte nodulation could effectively encase these filamentous cells and disable their infection. On the other hand, yeast cells, although vulnerable for phagocytosis, can effectively kill the infected larvae [36,42]. Surprisingly, yeast and hyphae can both be phagocytosed by murine macrophages, whereas no phagocytosis was observed for pseudohyphae (Fig. 2). In this case, cell surface molecules differentially presented on hyphae versus pseudohyphae might be more critical than the physical shape. Nonetheless, strains in both filamentous forms are incapable of disseminating from the lungs inmouse models and are consequently unable to cause fatal brain infections [20,36]. Thus, being in the yeast form is clearly advantageous for cryptococcal systemic spread in a mammalian host. Hence, as a facultative intracellular pathogen, resistance to phagocytosis is only part of the equation in determining the overall level of virulence of *Cryptococcus* in a multicellular host.

It is reasonable to assume that these different morphotypes differ in their cell surface composition or structure (protein and complex carbohydrates). For instance, Znf2 is known to control multiple cell surface factors in *Cryptococcus*, including proteins for cellular adhesion [20,21,55]. The effect of mutations in the RAM pathway on cryptococcal cell surface is unknown; however, these cells were not detected as adhered to macrophages. While grown on media with cell wall perturbing agents, the *ZNF2*$^{oe}$ strain (hyphae) showed the highest sensitivity to Caspofungin and Congo red, followed by the RAM mutant (pseudohyphae) and then the wild type (yeast) (Supplemental Fig. 2A). As Caspofungin inhibits (1–3)-$\beta$-D-glucan synthase and Congo red binds to $\beta$-1,4-glucans [57,58], this result suggests that *ZNF2* overexpression and RAM pathway mutantions affect the $\beta$-glucan to a different extent. Moreover, both hyphae and pseudohyphae were more sensitive to the cell wall and membrane disturbing detergent SDS than yeasts (Supplemental Fig. 2A). By constract, no gross difference in the production of chitin/chitosan or capsule between the yeast, hyphae, or pseudohyphae was detected through Calcofluor white and India ink staining (Supplemental Fig. 2B). However, these assays could not detect subtle changes in their composition or structure. Further detailed analyses of the cell wall of these morphotypes are warranted.

The physical size of the pathogen and of the phagocytes appears to be a critical factor for phagocytosis. For example, a previous study showed that haemocytes of *G. mellonella* are effective in phagocytosis of *Aspergillus fumigatus* conidia that are smaller than 3 micrometers [38]. Although we could easily detect phagocytosis of cryptococcal yeast cells of 3–5 micrometers by *G. mellonella* haemocytes (Fig. 5), it is relatively rare to observe phagocytosis of filaments [59]. Attempts to engulf and destroy filaments are often likely to be futile as we observed for amoebae (Fig. 3C). It is possible that *G. mellonella* resorts to and relies primarily on haemocyte nodulation for particles of larger sizes, like hyphae or

pseudohyphae (Fig. 5). What is surprising to us is that the J774A.1 macrophage, which is of similar size as the amoebae used in this study, can efficiently engulf cryptococcal hyphae (Fig. 2). It is unclear why macrophages failed to phagocytose pseudohyphae. Clustering of cells and/or lower adherence of the RAM mutant might be responsible for this phenomenon.

Differences in genotype, in addition to the variations in morphotype, also affect the outcome of the interaction between *Cryptococcus* and the host. For instance, yeast cells in the XL280 background are more resistant against amoebic predation than yeast cells in the H99 background (Fig. 4). This is contrary to their virulence level in mouse models [50,60]. Moreover, some yeasts might be digested and serve as a food source for amoebae ([61] and this study), while some other cryptococcal yeasts could revert that relationship and replicate inside amoebae after being phagocytosed [47]. In a murine model, alveolar macrophages could rapidly phagocytose yeast cells after the intratracheal infection [46]. However, yeast cells of some strains can adopt different strategies to avoid phagocytosis [62,63].

Often a microbial population grown under natural condition is not homogenous, even if the population is derived from a single parental cell. These cells could be heterogenous in cellular physiology, morphology, or size. The balance of different subpopulations could be shifted in response to different environmental stimuli, maximizing the community fitness or enhancing microbial survival under disparate conditions. Pigeon guano, a natural niche of *C. neoformans*, provides a stimulating environment for cryptocccal mating [64]. A cryptococcal mating colony, for example, contain yeasts, pseudohyphae, germ tubes, and hyphae. A subpopulation of the hyphae could further differentiate into fruiting bodies and generate recombinant progeny that are then distributed to new locations in the environment [43]. The stochasticity in gene expression in cells of the same morphotype and the dynamics in morphotype transition are part of the bet-hedging strategy of this fungus to survive under changing and unpredictable selective pressures. Thus, although it is important to understand the impact of a pure morphotype on the cellular interaction between cryptococcus and the host, it is equally important to extrapolate such findings to the population level with caution. Similarly, the interpretation of the interaction of *Cryptococcus* with multicellular hosts at the cellular level should be placed in the context of the host organism as a whole.

## Supplementary Material

Refer to Web version on PubMed Central for supplementary material.

## Acknowledgments

We thank Drs. Bing Zhai and Qingming Qin for their assistance with the macrophage experiments. We gratefully acknowledge the financial support from the National Institute of Allergy and Infectious Diseases (grants R21 AI094364 to A. I., R01 AI097599 and R21 AI107138 to X. L.). A. I. is supported on an Australian Research Council Future Fellowship. X. L. holds an Investigators in the Pathogenesis of Infectious Disease Award from the Burroughs Wellcome Fund. The funders had no role in study design, data collection and analysis, decision to publish, or preparation of the manuscript.

## References

1. Nemecek JC, Wuthrich M, Klein BS. Global control of dimorphism and virulence in fungi. Science. 2006; 312(5773):583–588. [PubMed: 16645097]

2. Holbrook ED, Rappleye CA. *Histoplasma capsulatum* pathogenesis: making a lifestyle switch. Curr Opin Microbiol. 2008; 11(4):318–324. [PubMed: 18573684]
3. Park BJ, Wannemuehler KA, Marston BJ, et al. Estimation of the current global burden of cryptococcal meningitis among persons living with HIV/AIDS. AIDS. 2009; 23(4):525–530. [PubMed: 19182676]
4. Casadevall, A.; Perfect, JR. Cryptococcus neoformans. Washington, DC: ASM Press; 1998.
5. Casadevall A, Steenbergen JN, Nosanchuk JD. 'Ready made' virulence and 'dual use' virulence factors in pathogenic environmental fungi—the *Cryptococcus neoformans* paradigm. Curr Opin Microbiol. 2003; 6(4):332–337. [PubMed: 12941400]
6. Lin X. *Cryptococcus neoformans*: morphogenesis, infection, and evolution. Infect Genet Evol. 2009; 9(4):401–416. [PubMed: 19460306]
7. Wang L, Lin X. Morphogenesis in fungal pathogenicity: shape, size, and surface. PLoS Pathogens. 2012; 8(12):e1003027. [PubMed: 23236274]
8. Sil A, Andrianopoulos A. Thermally dimorphic human fungal pathogens-polyphyletic pathogens with a convergent pathogenicity trait. Cold Spring Harb Perspect Med. 201410.1101/cshperspect.a019794
9. Neilson JB, Ivey MH, Bulmer GS. *Cryptococcus neoformans*: pseudohyphal forms surviving culture with *Acanthamoeba polyphaga*. Infect Iimmun. 1978; 20(1):262–266.
10. Zaragoza O, Nielsen K. Titan cells in *Cryptococcus neoformans*: cells with a giant impact. Curr Op in Microbiol. 2013; 16(4):409–413.
11. Zaragoza O, Garcia-Rodas R, Nosanchuk JD, et al. Fungal cell gigantism during mammalian infection. PLoS Pathogens. 2010; 6(6):e1000945. [PubMed: 20585557]
12. Okagaki LH, Strain AK, Nielsen JN, et al. Cryptococcal cell morphology affects host cell interactions and pathogenicity. PLoS Pathogens. 2010; 6(6):e1000953. [PubMed: 20585559]
13. Kwon-Chung KJ. A new genus, *Filobasidiella*, the perfect state of *Cryptococcus neoformans*. Mycologia. 1975; 67(6):1197–1200. [PubMed: 765816]
14. Alspaugh JA, Davidson RC, Heitman J. Morphogenesis of *Cryptococcus neoformans*. Contrib Microbiol. 2000; 5:217–238. [PubMed: 10863675]
15. Heitman J. Evolution of eukaryotic microbial pathogens via covert sexual reproduction. Cell Host & Microbe. 2010; 8(1):86–99. [PubMed: 20638645]
16. Kwon-Chung KJ. Morphogenesis of *Filobasidiella neoformans*, the sexual state of *Cryptococcus neoformans*. Mycologia. 1976; 68(4):821–833. [PubMed: 790172]
17. Lin X, Hull CM, Heitman J. Sexual reproduction between partners of the same mating type in *Cryptococcus neoformans*. Nature. 2005; 434(7036):1017–1021. [PubMed: 15846346]
18. Wickes BL, Mayorga ME, Edman U, et al. Dimorphism and haploid fruiting in *Cryptococcus neoformans*: association with the alpha-mating type. Proc Natl Acad Sci U S A. 1996; 93(14):7327–7331. [PubMed: 8692992]
19. Lin X, Huang JC, Mitchell TG, et al. Virulence attributes and hyphal growth of *C. neoformans* are quantitative traits and the *MAT*alpha allele enhances filamentation. PLoS Genetics. 2006; 2(11):e187. [PubMed: 17112316]
20. Wang L, Zhai B, Lin X. The link between morphotype transition and virulence in *Cryptococcus neoformans*. PLoS Pathogens. 2012; 8(6):e1002765. [PubMed: 22737071]
21. Wang L, Tian X, Gyawali R, et al. Fungal adhesion protein guides community behaviors and autoinduction in a paracrine manner. Proc Natl Acad Sci U S A. 2013; 110(28):11571–11576. [PubMed: 23798436]
22. Fu J, Morris IR, Wickes BL. The production of monokaryotic hyphae by *Cryptococcus neoformans* can be induced by high temperature arrest of the cell cycle and is independent of samesex mating. PLoS Pathogens. 2013; 9(5):e1003335. [PubMed: 23658522]
23. Lin X, Jackson JC, Feretzaki M, et al. Transcription factors Mat2 and Znf2 operate cellular circuits orchestrating opposite- and same-sex mating in *Cryptococcus neoformans*. PLoS Genetics. 2010; 6(5):e1000953. [PubMed: 20485569]

24. Zhai B, Zhu P, Foyle D, et al. Congenic strains of the filamentous form of *Cryptococcus neoformans* for studies of fungal morphogenesis and virulence. Infect Immun. 2013; 81(7):2626–2637. [PubMed: 23670559]
25. Wang L, Tian X, Gyawali R, et al. Morphotype transition and sexual reproduction are genetically associated in a ubiquitous environmental pathogen. PLoS Pathogens. 2014; 10(6):e1004185. [PubMed: 24901238]
26. Del Poeta M. Role of phagocytosis in the virulence of *Cryptococcus neoformans*. Eukaryotic Cell. 2004; 3(5):1067–1075. [PubMed: 15470235]
27. Lee SC, Phadke S, Sun S, Heitman J. Pseudohyphal growth of *Cryptococcus neoformans* is a reversible dimorphic transition in response to ammonium that requires Amt1 and Amt2 ammonium permeases. Eukaryotic Cell. 2012; 11(11):1391–1398. [PubMed: 23002105]
28. Walton FJ, Heitman J, Idnurm A. Conserved elements of the RAM signaling pathway establish cell polarity in the basidiomycete *Cryptococcus neoformans* in a divergent fashion from other fungi. Mol Biol Cell. 2006; 17(9):3768–3780. [PubMed: 16775005]
29. Maerz S, Seiler S. Tales of RAM and MOR: NDR kinase signaling in fungal morphogenesis. Curr Op inMicrobiol. 2010; 13(6):663–671.
30. Bogomolnaya LM, Pathak R, Guo J, et al. Roles of the RAM signaling network in cell cycle progression in *Saccharomyces cerevisiae*. Current Genetics. 2006; 49(6):384–392. [PubMed: 16552603]
31. Brace J, Hsu J, Weiss EL. Mitotic exit control of the *Saccharomyces cerevisiae* Ndr/LATS kinase Cbk1 regulates daughter cell separation after cytokinesis. Mol Cell Biol. 2011; 31(4):721–735. [PubMed: 21135117]
32. Nelson B, Kurischko C, Horecka J, et al. RAM: a conserved signaling network that regulates Ace2p transcriptional activity and polarized morphogenesis. Mol Biol Cell. 2003; 14(9):3782–3803. [PubMed: 12972564]
33. Du LL, Novick P. Pag1p, a novel protein associated with protein kinase Cbk1p, is required for cell morphogenesis and proliferation in *Saccharomyces cerevisiae*. Mol Biol Cell. 2002; 13(2):503–514. [PubMed: 11854408]
34. Bidlingmaier S, Weiss EL, Seidel C, et al. The Cbk1p pathway is important for polarized cell growth and cell separation in *Saccharomyces cerevisiae*. Mol Cell Biol. 2001; 21(7):2449–2462. [PubMed: 11259593]
35. Racki WJ, Becam AM, Nasr F, et al. Cbk1p, a protein similar to the human myotonic dystrophy kinase, is essential for normal morphogenesis in *Saccharomyces cerevisiae*. EMBO J. 2000; 19(17):4524–4532. [PubMed: 10970846]
36. Magditch DA, Liu TB, Xue C, et al. DNA mutations mediate microevolution between host-adapted forms of the pathogenic fungus *Cryptococcus neoformans*. PLoS Pathogens. 2012; 8(10):e1002936. [PubMed: 23055925]
37. Colman-Lerner A, Chin TE, Brent R. Yeast Cbk1 andMob2 activate daughter-specific genetic programs to induce asymmetric cell fates. Cell. 2001; 107(6):739–750. [PubMed: 11747810]
38. Renwick J, Daly P, Reeves EP, et al. Susceptibility of larvae of *Galleria mellonella* to infection by *Aspergillus fumigatus* is dependent upon stage of conidial germination. Mycopathologia. 2006; 161(6):377–384. [PubMed: 16761185]
39. Kechichian TB, Shea J, Del Poeta M. Depletion of alveolar macrophages decreases the dissemination of a glucosylceramidedeficient mutant of *Cryptococcus neoformans* in immunodeficient mice. Infect Immun. 2007; 75(10):4792–4798. [PubMed: 17664261]
40. Charlier C, Nielsen K, Daou S, et al. Evidence of a role for monocytes in dissemination and brain invasion by *Cryptococcus neoformans*. Infect Immun. 2009; 77(1):120–127. [PubMed: 18936186]
41. Sabiiti W, Robertson E, Beale MA, et al. Efficient phagocytosis and laccase activity affect the outcome of HIV-associated cryptococcosis. J Clin Investigat. 2014; 124(5):2000–2008.
42. Mylonakis E, Moreno R, ElKhoury JB, et al. *Galleria mellonella* as a model system to study *Cryptococcus neoformans* pathogenesis. Infect Iimmun. 2005; 73(7):3842–3850.
43. Upadhyay S, Torres G, Lin X. Laccases involved in 1,8-dihydroxynaphthalene melanin biosynthesis in *Aspergillus fumigatus* are regulated by developmental factors and copper homeostasis. Eukaryotic Cell. 2013; 12(12):1641–1652. [PubMed: 24123270]

44. Ory JJ, Griffith CL, Doering TL. An efficiently regulated promoter system for *Cryptococcus neoformans* utilizing the *CTR4* promoter. Yeast. 2004; 21(11):919–926. [PubMed: 15334556]
45. Herth W, Schnepf E. The fluorochrome, calcofluor white, binds oriented to structural polysaccharide fibrils. Protoplasma. 1980; 105(1–2):129–133.
46. Feldmesser M, Kress Y, Novikoff P, et al. *Cryptococcus neoformans* is a facultative intracellular pathogen in murine pulmonary infection. Infect Immun. 2000; 68(7):4225–4237. [PubMed: 10858240]
47. Steenbergen JN, Shuman HA, Casadevall A. *Cryptococcus neoformans* interactions with amoebae suggest an explanation for its virulence and intracellular pathogenic strategy in macrophages. Proc Natl Acad Sci U S A. 2001; 98(26):15245–15250. [PubMed: 11742090]
48. Kwon-Chung KJ, Fraser JA, Doering TL, et al. *Cryptococcus neoformans* and *Cryptococcus gattii*, the etiologic agents of cryptococcosis. Cold Spring Harb Perspect Med. 2014; 4(7):a019760. [PubMed: 24985132]
49. Casadevall A. Amoeba provide insight into the origin of virulence in pathogenic fungi. Adv Exp Med Biol. 2012; 710:1–10. [PubMed: 22127880]
50. Nielsen K, Cox GM, Wang P, et al. Sexual cycle of *Cryptococcus neoformans* var. *grubii* and virulence of congenic a and alpha isolates. Infect Immun. 2003; 71(9):4831–4841. [PubMed: 12933823]
51. Mak P, Zdybicka-Barabas A, Cytrynska M. A different repertoire of *Galleria mellonella* antimicrobial peptides in larvae challenged with bacteria and fungi. Dev Comp Immunol. 2010; 34(10):1129–1136. [PubMed: 20558200]
52. Lavine MD, Strand MR. Insect hemocytes and their role in immunity. Insect Biochem Mol Biol. 2002; 32(10):1295–1309. [PubMed: 12225920]
53. Cytrynska M, Mak P, Zdybicka-Barabas A, et al. Purification and characterization of eight peptides from *Galleria mellonella* immune hemolymph. Peptides. 2007; 28(3):533–546. [PubMed: 17194500]
54. Lavine MD, Strand MR. Insect hemocytes and their role in immunity. Insect Biochem Mol Biol. 2002; 32(10):1295–1309. [PubMed: 12225920]
55. Bogus MI, Kedra E, Bania J, et al. Different defense strategies of *Dendrolimus pini*, *Galleria mellonella*, and *Calliphora vicina* against fungal infection. J Insect Physiol. 2007; 53(9):909–922. [PubMed: 17512001]
56. Strand MR, Pech LL. Immunological basis for compatibility in parasitoid-host relationships. Ann Rev Entomol. 1995; 40:31–56. [PubMed: 7810989]
57. Wood PJ, Fulcher RG. Dye interactions. A basis for specific detection and histochemistry of polysaccharides. J Histochem Cytochem. 1983; 31(6):823–826. [PubMed: 6841974]
58. Deresinski SC, Stevens DA. Caspofungin. Clin Infect Dis. 2003; 36(11):1445–1457. [PubMed: 12766841]
59. Jackson JC, Higgins LA, Lin X. Conidiation color mutants of *Aspergillus fumigatus* are highly pathogenic to the heterologous insect host *Galleria mellonella*. PloS One. 2009; 4(1):e4224. [PubMed: 19156203]
60. Perfect JR, Lang SD, Durack DT. Chronic cryptococcal meningitis: a new experimental model in rabbits. Am J Pathol. 1980; 101(1):177–194. [PubMed: 7004196]
61. Bunting LA, Neilson JB, Bulmer GS. *Cryptococcus neoformans*: gastronomic delight of a soil ameba. Sabouraudia. 1979; 17(3):225–232. [PubMed: 394365]
62. Luberto C, Martinez-Marino B, Taraskiewicz D, et al. Identification of App1 as a regulator of phagocytosis and virulence of *Cryptococcus neoformans*. J Clin Invest. 2003; 112(7):1080–1094. [PubMed: 14523045]
63. Kozel TR, Gotschlich EC. The capsule of *Cryptococcus neoformans* passively inhibits phagocytosis of the yeast by macrophages. J Immunol. 1982; 129(4):1675–1680. [PubMed: 7050244]
64. Nielsen K, De Obaldia AL, Heitman J. *Cryptococcus neoformans* mates on pigeon guano: implications for the realized ecological niche and globalization. Eukaryotic Cell. 2007; 6(6):949–959. [PubMed: 17449657]

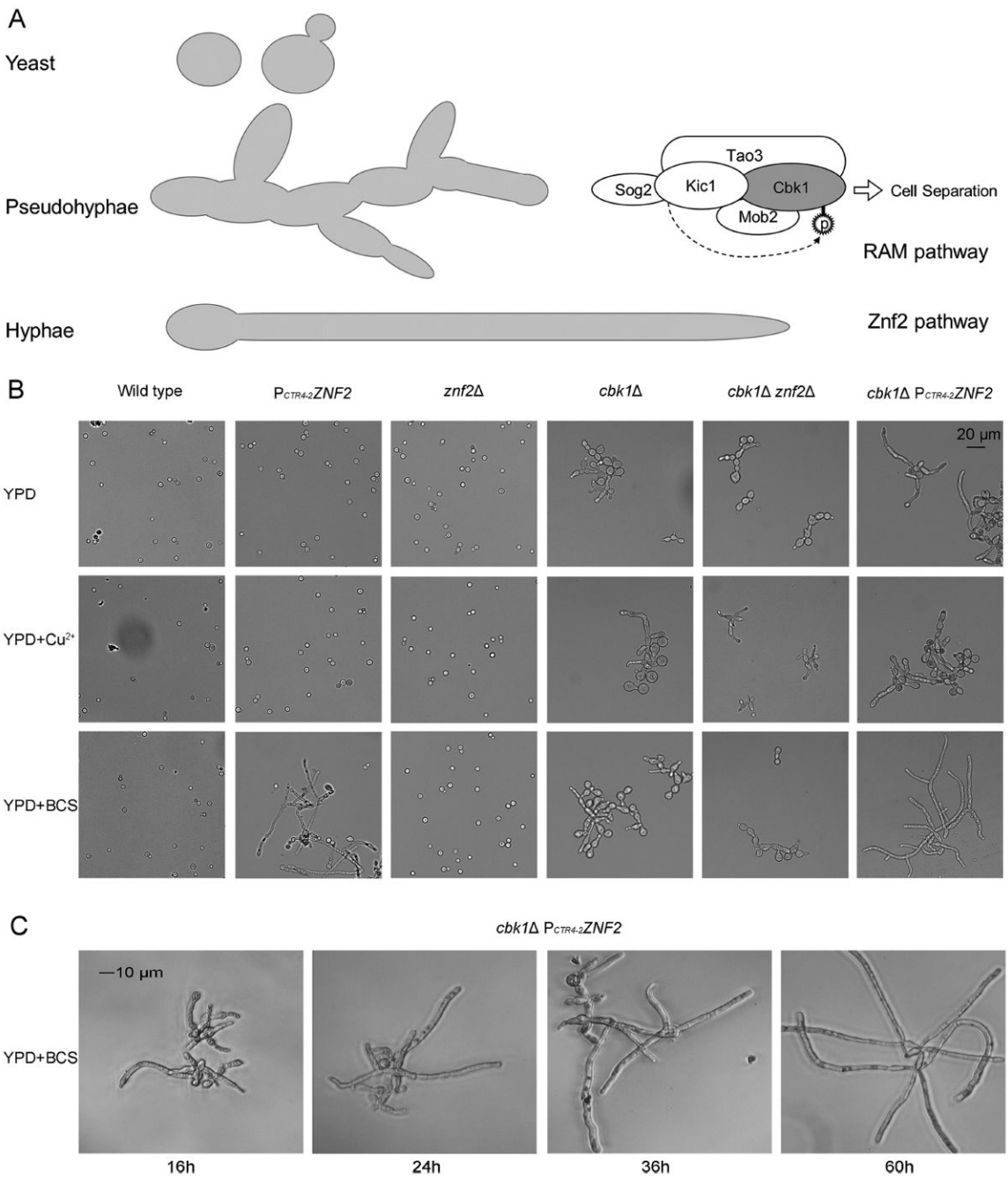


**Figure 1.**

The Znf2 and the RAM pathways control distinct aspects of morphogenesis. (**A**) Diagram of the three morphotypes of *Cryptococcus* and the Znf2 and RAM pathways. The five RAM pathway components, Cbk1, Kic1, Mob2, Tao3, and Sog2, are depicted, with Cbk1 being the ultimate kinase of this complex [28]. Znf2 is a master activator of filamentation. (**B**) The cellular morphology of the wild-type H99 strain, the $P_{CTR4\text{-}2}$*ZNF2* strain, the *znf2*Δ mutant, the *cbk1*Δ mutant, the *cbk1*Δ *znf2*Δ double mutant, and the *cbk1*Δ $P_{CTR4\text{-}2}$*ZNF2* strain was examined from cultures in YPD, YPD+copper, and YPD+BCS media. (**C**) The cellular

morphology of the *cbk1*Δ $P_{CTR4\text{-}2}$*ZNF2* strain was examined microscopically after the induction of *ZNF2* expression for the indicated time periods.

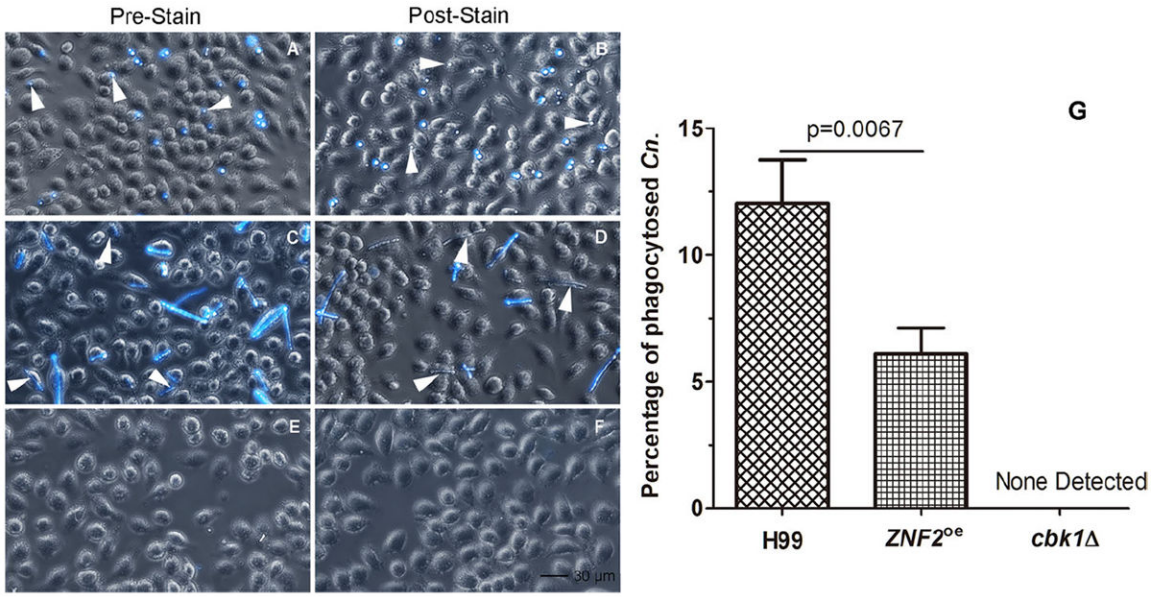


**Figure 2.**

Phagocytosis of cryptococcal cells of different morphology by murine macrophage cells. Murine J774A.1 cells were infected by *C. neoformans* wild-type strain H99 (A, B), the $P_{CTR4\text{-}2}$*ZNF2* strain (C, D), and the *cbk1*Δ mutant (E, F) for two hours and then fixed. The left panel images were taken with cryptococcal cells stained with calcofluor white prior to the infection (A, C, E). The right panel images were taken with the co-culture stained with calcofluor white after phagocytosis (B, D, F). Statistical analysis was performed on the percentage of phagocytosed *C. neoformans* (*Cn*) cells (G). A *p* value lower than .05 is considered statistically significant. No *cbk1*Δ mutant cells were phagocytosed and thus no fluorescent signal was detected.

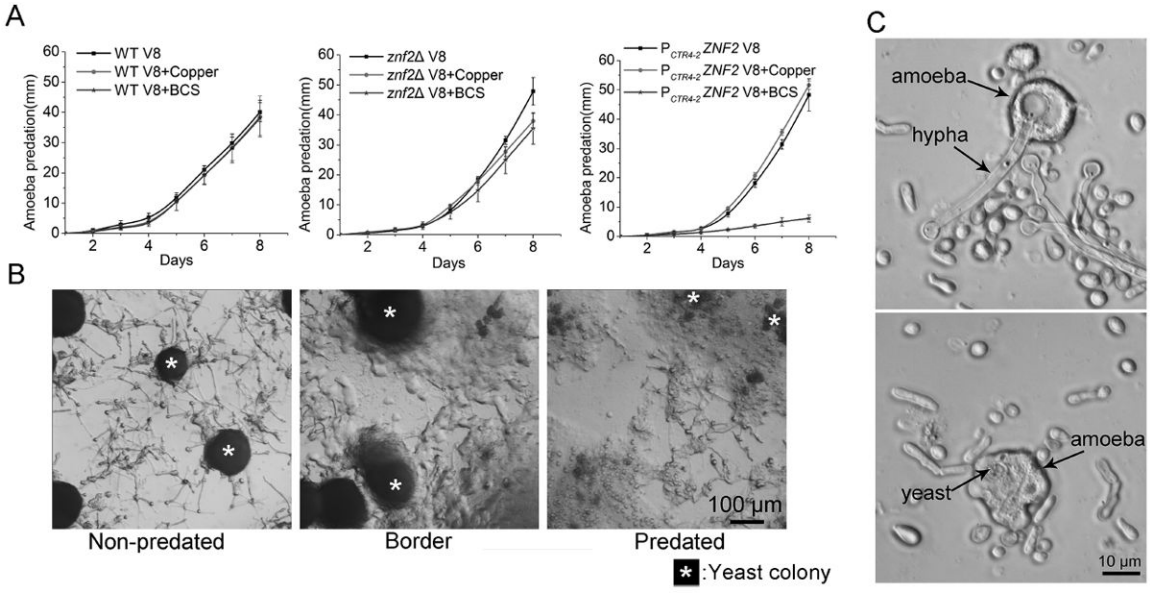


**Figure 3.**

Amoebic predation of *Cryptococcus*. (**A**) The dynamics of amoebic predation of *Cryptococcus* wild-type strain H99, the *znf2*Δ mutant, and the $P_{CTR4\text{-}2}$*ZNF2* strain on V8 juice agar, V8+copper, and V8+BCS was recorded for 8 days. No expansion of predation zone on the *cbk1*Δ mutant was observed even after three weeks (not shown). (**B**) The area outside of the predation zone, at the front of the predation, and inside the predation zone of the $P_{CTR4\text{-}2}$*ZNF2* strain on V8+BCS agar medium. * indicate the yeast colonies. (**C**) From the predation zone of the $P_{CTR4\text{-}2}$*ZNF2* strain on V8+BCS agar medium, amoebae with attempts to phagocytose hyphae were observed (upper image) and amoebae with completely phagocytosed yeast cells were observed (lower image).

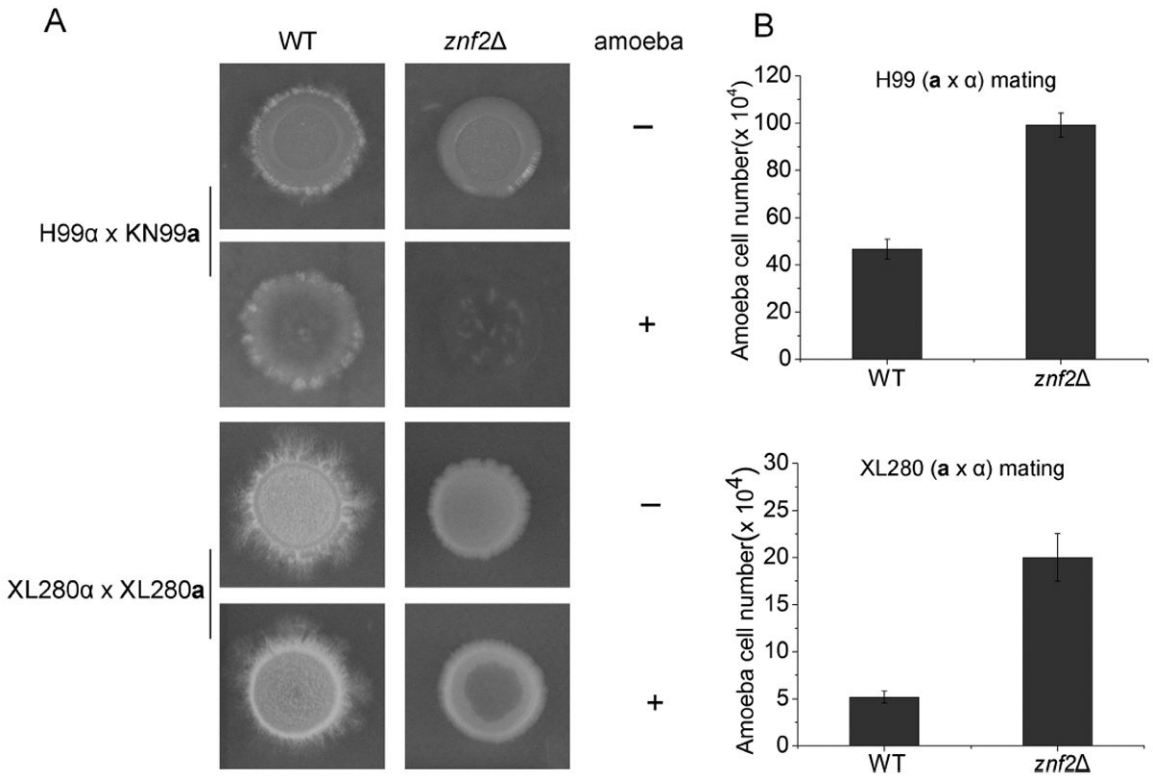


**Figure 4.**

Amoebic predation of mating colonies. (**A**) The wild-type strain pairs (H99$\alpha$ × KN99**a** and XL280$\alpha$ × XL280**a**) and their corresponding *znf2*Δ mutant pairs were mated on V8 medium. The images of intact colonies and colonies with amoebae predation are shown. (**B**) Amoebae cells recovered from the mating colonies were quantified.

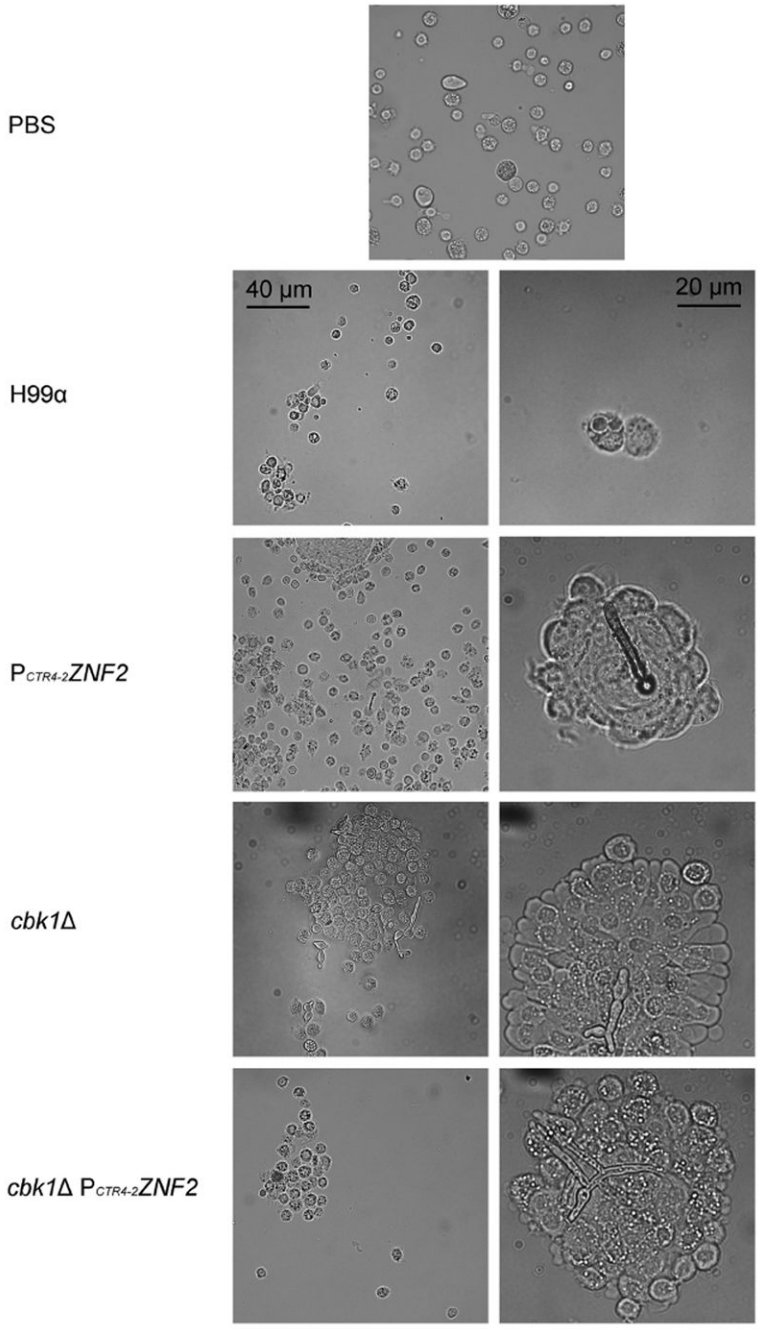


**Figure 5.**

*Galleria mellonella* haemocyte nodulation induced by cryptococcal infections. Larvae were infected with cryptococcal cells (wildtype H99, the *znf2*Δ mutant, and the $P_{CTR4\text{-}2}$*ZNF2* strain) precultured overnight in YPD+BCS liquid medium. Haemolymph from infected larvae was collected at 4 hours post inoculation and was immediately observed microscopically.

**Table 1**

Morphotype affects the interaction between *C. neoformans* and its hosts.

| | **Yeast** | **Pseudohyphae** | **Hyphae** |
|---|---|---|---|
| *Acanthamoeba castellanii* | Phagocytosed | Survived | Survived |
| *Galleria mellonella* | Phagocytosed | Contained by aggregated haemocytes | Contained by aggregated haemocytes |
| Murine macrophage cell J774A.1 | Phagocytosed | No adherence or phagocytosis | Phagocytosed |